



Norwegian University of
Science and Technology

Vapor-Liquid equilibrium in DEEA/H₂O/ CO₂ system; Experiments and modeling

Syed Amjad Hussain Zaidy

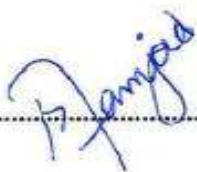
Chemical Engineering

Submission date: June 2011

Supervisor: Hallvard Fjøsne Svendsen, IKP

DECLARATION

I declare that this is an independent work according to the exam regulations of the Norwegian University of Science and Technology.

Date and signature:  27-06-2011

Acknowledgements

All praise goes to **Almighty Allah** Who is the creator of this universe. I'm thankful to **Department of Chemical Engineering (NTNU)** and **SINTEF** for providing me facilities for the completion of my work.

I'm thankful to my supervisors **Professor Hallvard F.Svendsen**, **Dr.Ardi Hartono** and **Mr.Ugochukwu E.Aronu** for their help and guidance through the project period. Their enthusiasm on the topic of carbon capture has been a great inspiration to me. The report forms a part of icap project. I also thank all my friends with whom I have had honor of sharing memorable moments and experiences in the last 2 years.

Finally, I wish to express my deepest thankfulness and love to all my family members for their endless support throughout my work.

Syed Amjad Hussain Zaidy

Abstract

Experiment data for vapor-liquid equilibrium (VLE) of CO₂ were conducted for DEEA 5M and 2M. The study was performed in two VLE apparatuses from 40 to 120 °C with atmospheric VLE apparatus and high pressure VLE apparatus. The extended UNIQUAC model framework was applied and the model parameters were fitted with experimental data with partial pressure of CO₂ for atmospheric VLE and total pressure with high pressure VLE apparatus. Modfit was applied for further optimization. The model predictions are good and give an average absolute relative deviation (AARD) of 26.5 %. Further the model predicted speciation results seems logical. Parity plots were used to show the deviation between the experimental values and model predicted values. Predictions from UNIQUAC for binary system were compared with Raoult's law to look for deviations.

Table of Contents

Declaration	
Acknowledgements	
Abstract	
Table of contents	
1.0 Introduction	1
1.1 Carbon capture and storage	2
1.2 CO ₂ capture techniques	3
1.2.1 Precombustion Capture	4
1.2.2 Postcombustion Capture	4
1.2.3 Oxyfuel combustion Capture	4
1.3 Basic chemistry and kinetics of amines	5
1.3.1 Primary amines	5
1.3.2 Secondary amines	5
1.3.3 Tertiary amines	6
1.4 Sterically hindered amines	7
1.5 Motivation and scope of work	8
2.0 Experimental techniques	10
2.1 Materials	10
2.1.1 Solutions and calibration gases	10
2.1.2 Chemicals for CO ₂ analysis and amine analysis	10
2.2 Experimental setup	11
2.2.1 pKa measurements	11
2.2.2 Atmospheric or low pressure VLE apparatus	12
2.2.3 High pressure and high temperature VLE apparatus	14
2.2.4 CO ₂ analysis and amine analysis of liquid samples	15
2.3 Calibration of analyzers	15
2.3.1 High pressure equipment	15
2.3.2 Low pressure equipment	16

3.0	Experimental results and discussion	17
3.1	Dissociation constants or pKa results	20
4.0	Thermodynamic framework	21
4.1	The equilibria involved	21
4.2	The extended UNIQUAC model	24
4.3	Activity coefficient model	25
4.4	Parameter regression	26
4.5	Thermodynamic parameters	27
5.0	Modeling results and discussion	29
5.1	Binary DEEA-H ₂ O system	29
5.2	Ternary CO ₂ -DEEA-H ₂ O system	31
5.3	Speciation	35
	Conclusions	38
	Future recommendations	39
	References	40
	Acronyms and abbreviations	42
	List of symbols and units	43
	Appendices	45

1.0 Introduction

Global rise in temperature during the last ten decades and growing concern about the environment and global warming have started a new era of research and development. Increase in the anthropogenic sources is considered to be the major cause of global warming. Carbon dioxide is considered primary green house gas causing environmental problems. Assessing CO₂ capture and storage requires a comprehensive delineation of CO₂ sources. The choice of capture source depends on its volume, concentration and partial pressure, integrated system aspects, and its proximity to a suitable reservoir. CO₂ is emitted from a number of sources, mainly from fossil fuel combustion for power generation, industrial use, residential use and transport sector. In some sectors like power generation and industrial sectors, many sources have large volumes of CO₂, which make them suitable for CO₂ capture. Meanwhile large number of small point and, in the case of transport, mobile sources characterize the other sector, making them less suitable for CO₂ capture. (IPCC report, 2005)

Source	CO ₂ concentration % vol (dry)	Pressure of gas stream MPa ^a	CO ₂ partial pressure MPa
CO₂ from fuel combustion			
• Power station flue gas:			
Natural gas fired boilers	7 - 10	0.1	0.007 - 0.010
Gas turbines	3 - 4	0.1	0.003 - 0.004
Oil fired boilers	11 - 13	0.1	0.011 - 0.013
Coal fired boilers	12 - 14	0.1	0.012 - 0.014
IGCC ^b : after combustion	12 - 14	0.1	0.012 - 0.014
• Oil refinery and petrochemical plant fired heaters	8	0.1	0.008
CO₂ from chemical transformations + fuel combustion			
• Blast furnace gas:			
Before combustion ^c	20	0.2 - 0.3	0.040 - 0.060
After combustion	27	0.1	0.027
• Cement kiln off-gas	14 - 33	0.1	0.014 - 0.033
CO₂ from chemical transformations before combustion			
• IGCC: synthesis gas after gasification	8 - 20	2 - 7	0.16 - 1.4

^a 0.1 MPa = 1 bar.

^b IGCC: Integrated gasification combined cycle.

^c Blast furnace gas also contains significant amounts of carbon monoxide that could be converted to CO₂ using the so-called shift reaction.

Table 1.1: properties of candidate gas streams that can be input to a capture process (sources: Campbell et al., 2000; Gielen and Moiguchi, 2003; Foster Wheeler, 1998; IEA GHG, 1999; IEA GHG, 2002a).

Technological changes in the production and nature of transport fuels, however, may eventually allow the capture of CO₂ from energy use also in this sector. Over 7,500 large CO₂ emission sources (above 0.1 Mt -CO₂ yr⁻¹) have been identified. These sources are distributed geographically around the world but four clusters of emissions can be observed: in North America (the Midwest and the eastern seaboard of the USA), North West Europe, South East Asia (eastern coast) and Southern Asia (the Indian sub-continent). Projections for the future (up to 2050) indicate that the number of emission sources from the power and industry sectors is likely to increase, predominantly in Southern and South East Asia, while the number of emission sources suitable for capture and storage in regions like Europe may decrease slightly.

Majority of the emission sources have concentrations of CO₂ typically lower than 15%. However, a small proportion (less than 2%) has concentrations that exceed 95%, making them more suitable for CO₂ capture. The high content sources are more economical to capture CO₂ from as compared to sources to low content sources because only dehydration and compression is required. **(IPCC report, 2005)**

1.1 Carbon capture and storage

Carbon capture and storage is considered the only best solution for decreasing CO₂ concentration in the atmosphere.

CO₂ capture plants were built and operating with removal of CO₂ from natural gas and synthesis gas during the 1970s and 1980s. CO₂ was also captured from the flue gas in a number of plants that were built in this time period in order to provide CO₂ for enhanced oil recovery (EOR). One can say the technology for the CO₂ from gas streams was available at the time the idea of CCS emerged. **(Bolland Olav compendium, 2010)**

One of the main reasons for CO₂ capture is to provide a concentrated stream of CO₂ which can further be transported and stored for instance underground. Capture technologies also open a way for low carbon or carbon free electricity and fuels for transportation. The energy required to operate CO₂ capture systems reduces the overall efficiency of power generation or other processes, leading to increased fuel requirements, solid wastes and environmental impacts relative to the same type of base plant without capture. However, as more efficient plants with

capture become available and replace many of the older less efficient plants now in service, the net impacts will be compatible with clean air emission goals for fossil fuel use. Minimization of energy requirements for capture, together with improvements in the efficiency of energy conversion processes will continue to be high priorities for future technology development in order to minimize overall environmental impacts and cost. (IPCC report, 2005)

1.2 CO₂ capture techniques

The fundamental chemical process involved in the generation of power from carbon-based fuel is the exothermic oxidation of carbon and since CO₂ is the lowest energy endpoint of oxidative reaction chain; its production is unavoidable. The elimination of carbon from power plant emission therefore requires either. (Stephen A. Rackley, 2010)

- Decarbonation of the fuel prior to combustion (pre-combustion capture)
- Separation of CO₂ from the products of combustion (post-combustion capture)
- Reengineering the combustion process to produce CO₂ as a pure combustion product (oxyfueling or oxyfuel combustion)

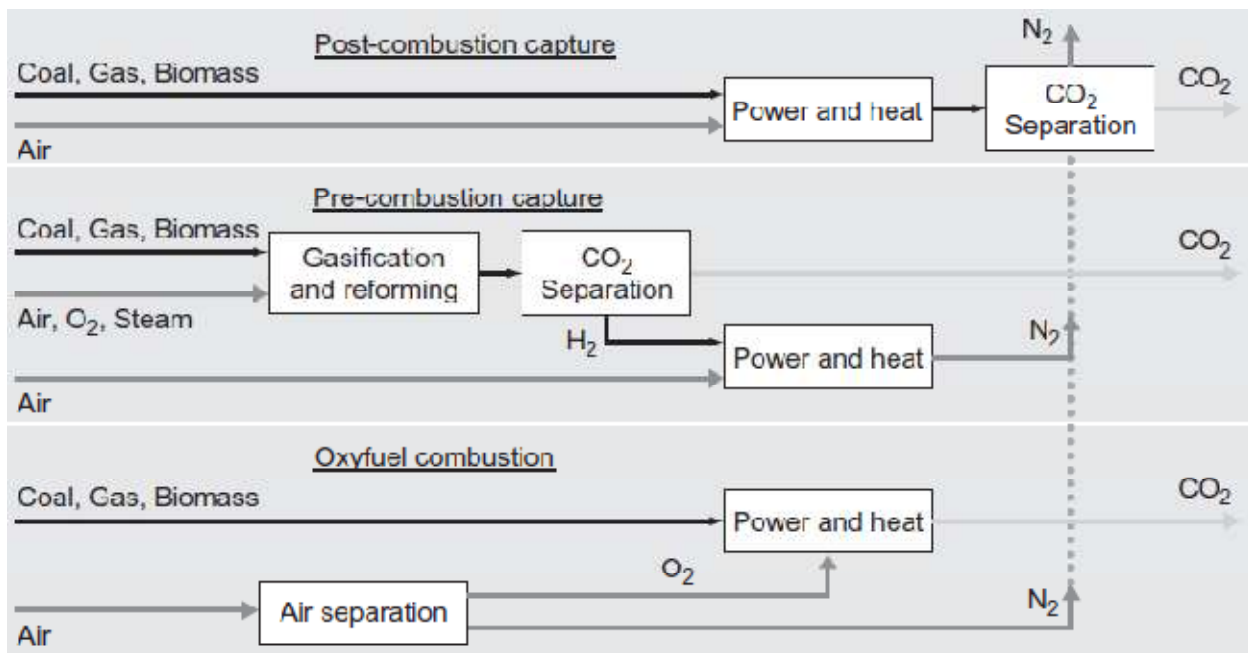


Figure 1.2: Options for CO₂ from power generation (Stephen A. Rackley, 2010)

Figure above shows the basic principle for three capture techniques.

1.2.1 Precombustion capture

Decarbonation of fuel like coal or biomass by gasification to produce hydrogen through a combination of partial combustion, reforming and water-gas shift, and the separation of CO₂ from the resulting reaction product stream. (Stephen A.Rackley, 2010)

1.2.2 Postcombustion capture

In this capture technique CO₂ is removed from the combustion product stream (flue gas) before emitted to atmosphere. This is an extension of the flue gas treatment for NO_x and SO_x removal, made more challenging by the relatively higher quantities of CO₂ in the gas stream (typically 5-15 % depending on fuel type used). (Stephen A.Rackley, 2010)

The startup for CO₂ test centre Mongstad is scheduled in 2011. The process description is shown in fig 1.3.

1.2.3 Oxyfuel combustion capture

It requires the delivery of oxygen rather than air to the combustion chamber, the gaseous product is nearly pure CO₂ rather than mixture which means no separation is required after combustion. Oxygen can be supplied as a gas stream or it can be done by separation from air or as a solid oxide in a chemical looping process. (Stephen A.Rackley, 2010)

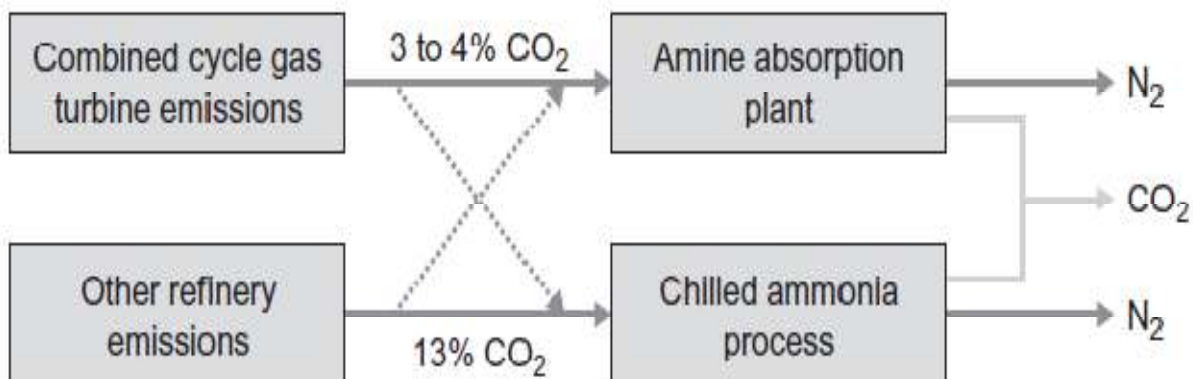


Figure 1.3: European CO₂ test centre Mongstad configuration (Stephen A.Rackley, 2010)

1.3 Basic chemistry and kinetics of amines

Generally alkanolamines amines have one hydroxyl group and one amino group. In general it can be considered that the hydroxyl group serves to reduce the vapor pressure and increases solubility in water, while the amino group provides the necessary alkalinity in water solutions to cause the absorption of acidic gases

Each alkanolamine has at least one hydroxyl group and one amino group. (Kohl Nielsen, 1997)

There are mainly three class of amine

1.3.1 Primary amines

Amines which have two hydrogen atoms directly attached to a nitrogen atom, such as MEA (monoethanolamine) and 2-(2-aminoethoxy) ethanol (DGA), are primary amines and are generally the most alkaline. (Kohl Nielsen, 1997)

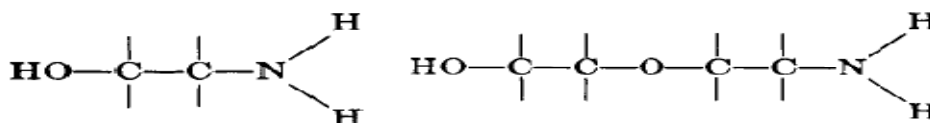


Figure 1.4: Primary amines MEA (left) and DGA (right) (Kohl Nielsen, 1997)

1.3.2 Secondary amines

Amines in which there is only one hydrogen attached to nitrogen for example diethanolamine (DEA) and di-isopropanolamine (DIPA). (Kohl Nielsen, 1997)

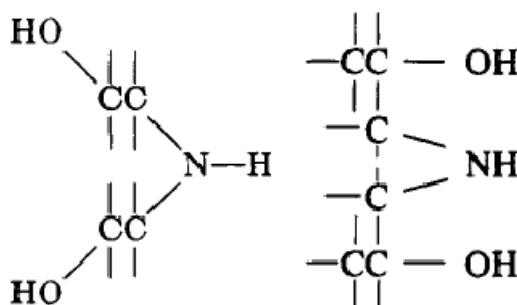


Figure 1.5: Secondary amines DEA (left) and DIPA (right) (Kohl Nielsen, 1997)

1.3.3 Tertiary amines

Tertiary amines represent completely substituted ammonia molecules with no hydrogen atoms attached to the nitrogen for example triethanolamine (TEA) and methyldiethanolamine (MDEA).

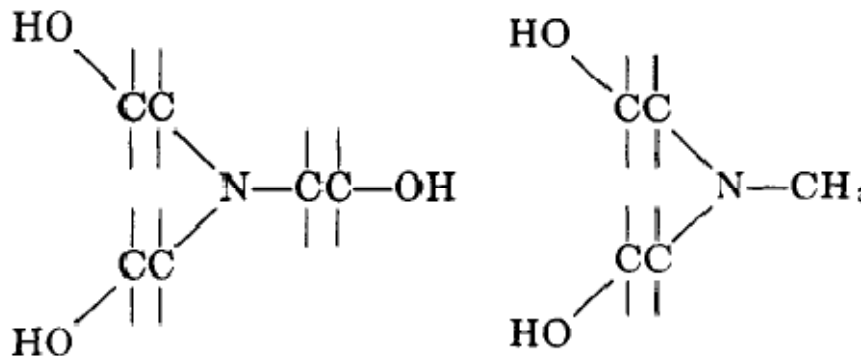


Figure 1.6: Tertiary amines TEA (left) and MDEA (right) (Kohl Nielsen, 1997)

Reactions occurring between solutions of primary amines like MEA with CO₂ and H₂S can be represented follows.

Ionization of water



Ionization of dissolved H₂S



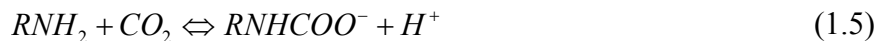
Hydrolysis and ionization of dissolved CO₂



Protonation of alknolamine



Carbamate formation



Reactions 1.1, 1.3, 1.4 and 1.5 are related to the principal species in aqueous alkaline treating solutions. Alternate pathways maybe selected for reactions relating the same species. A part from the species mentioned above there may be more species but here those species or reactions are shown that are important in absorption/desorption process.

Since all the reactions above are followed by specifically primary amines for example MEA but they can be applied to secondary amines as well by modifying the amine formula. Tertiary amine solutions undergo reactions 1.1 to 1.4 but they cannot react with CO₂ directly to form carbamates by reaction 1.5.

Since the equilibrium concentration of molecular H₂S and CO₂ in solution are proportional to their partial pressures in the gas phase (Henry's law) so the reactions 1.2, 1.3 and 1.5 are driven to the right by increased acid gas partial pressure. The reaction equilibria are also sensitive to temperature, causing the vapor pressure of the absorbed gases to increase as the temperature is increased. That is why it is possible to strip off gases with the application of heat.

If the reaction of equation 1.5 is predominant, as with primary amines, the carbamate ion ties up with an alkanolammonium ion through equation 1.4 and the capacity of the solution for CO₂ is limited to approximately 0.5 mole of CO₂ per mole of amine, even at high partial pressures of CO₂. This is because high stability of carbamate and its low rate of hydrolysis to bicarbonate. Meanwhile with tertiary amines which are unable to form carbamate can theoretically achieve higher loadings than primary amines. However amines do not form carbamate are slow in reaction rates. That is why these amines are used with activator (typically amine), responsible for increasing rate of hydration of dissolved CO₂. (**Kohl Nielsen, 1997**)

1.4 Sterically hindered amines

In a hindered amine a bulky alkyl group is attached to the amino group. Moreover it can be specifically defined by these two classes: (**Sartori and Savage, 1983**)

- 1) A primary amine in which the amino group is attached to a tertiary carbon

- 2) A secondary amine in which amino group is attached to at least one secondary or tertiary carbon

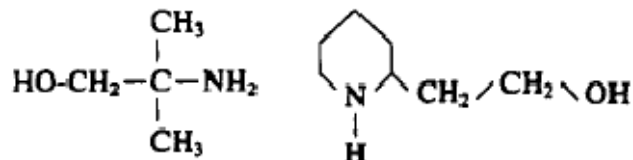


Figure 1.6: Sterically hindered amines 2-amino-2-methyl-1-propanol (AMP) (left) and 2-piperidine ethanol (PE) (right) (Kohl Nielsen, 1997)

Generally only aliphatic and cycloaliphatic amines are suitable for gas treating. Some amines like aromatic amines because of their low basicity lead to low absorption capacities and rates. A part from amino group and amines must contain another functional group to increase the solubility and reduce volatility for example a hydroxyl or carboxyl group. (Sartori and Savage, 1983)

Hindered amines have low carbamate stability than conventional amines like MEA. (Sartori and Savage, 1983)

1.5 Motivation and scope of work

Environmental problems caused by CO₂ emissions are increasing day by day. This is why engineers and scientists are providing indigenous ideas in order to solve this problem of CO₂ emission. CO₂ capture with amines is considered to become mature enough to be implemented in coal fired power plants. Some technical problems are necessary to be solved to make this economically feasible prominently energy reduction of energy requirement used for regeneration. In that context this thesis reflects the studies of solvent DEEA for CO₂ capture. DEEA has the following properties being a tertiary amine.

- High capacity (loading)
- Low heat/energy requirement for regeneration
- Low heat of reaction

Since DEEA is a tertiary amine that is why the Pco₂ depends on the amine concentration because of no carbamate which will be discussed later that is why it covers a whole range of loading with

concentrations 2M and 5M starting with very low 0.005 mol CO₂/mol DEEA to loadings of 1 mol CO₂/mol DEEA. But there are some problems with this solvent like low reaction rate which makes it not suitable to use because if used without promoter makes the height of absorption tower extremely tall. DEEA is relatively volatile and foams as compared to MEA, which requires an efficient design of water wash unit and foaming creates mass transfer or operational problems. These properties make it difficult to use solely. Study of DEEA is involved as two phase system as well with MAPA, with bottom phase with high loading (rich phase) and upper phase with low loading (lean phase), which is part of icap project.

Since energy reduction is the main target in CO₂ capture, so it is impossible to neglect tertiary amines. DEEA will most probably show some tremendous results when used with suitable promoters for instance MAPA.

2.0 Experimental Techniques

2.1 Materials

2.1.1 Solutions and calibration gases

DEEA(2-(Diethylamino)ethanol) with cas no 100-37-8 is sold under different brand names by Sigma Aldrich, the one used in these experiments has purity of greater than 99 % (fluka). DEEA 5M (61.14 wt %) and 2M (23.69 wt %) were prepared by using de-ionized water with great care. There might be impurities that can react with CO₂ but still since the purity is high so impurities have no significant effect. The CO₂ (purity > 99 mol % from AGA Gas GmbH) and Nitrogen N₂ (purity > 99.999 mol % from YARA PRAXAIR) were used for calibration, flushing and loading.

Calibration gases (4.96 mol % CO₂ from AGA Gas GmbH and 100ppm from YARA PRAXAIR) were used to calibrate the IR CO₂ analyzers of atmospheric pressure equipment before using them each time or on daily basis and flushing them with N₂ after finishing experiments for the day.

2.1.2 Chemicals for CO₂ analysis and amine analysis

Standard Solutions

0.1N NaOH (ampoule for 1000 mL supplied Merck KGaA)

0.1N HCl (ampoule for 1000 mL supplied Merck KgaA)

0.2N H₂SO₄ (2, 0.1 ampoules for 1000 mL supplied by Merck KgaA)

0.1N BaCl₂ (244 g BaCl₂.2H₂O/2L with purity > 99 % supplied by SIGMA-ALDRICH)

All standard solutions were prepared from above mentioned chemicals and de-ionized water.

Filters 0.45µmHAWP supplied by MILLIPORE

2.2 Experimental setup

2.2.1 pK_a measurement

Protonation constants for DEEA were measured over a wide temperature range of temperature wide range of temperature from 20 to 80 ° C.



Figure 2.1:G20 compact titrator, Mettler Toledo. (Kim et al, 2010)

The dissociation constant (pK_a) of DEEA was determined as the pH at half neutralization. Figure 2.1 shows the assembly of the apparatus. Parallel measurements were carried out using a computer controlled Mettler Toledo G20 compact titrator with a DGi115-SC pH glass electrode (uncertainty ± 0.02 pH) that dispenses 0.1 M HCl against 40 cm³ 0.01 M DEEA solution while data were logged online. Temperatures were kept constant ($\pm 0.1^\circ\text{C}$) during the titration experiments using a JULABO M4 oil bath. Electrode was calibrated each time at pH 4, 7 and 11 at temperature at which the experiment has to be performed. Titration curves at different temperature are shown in figure 2.2.

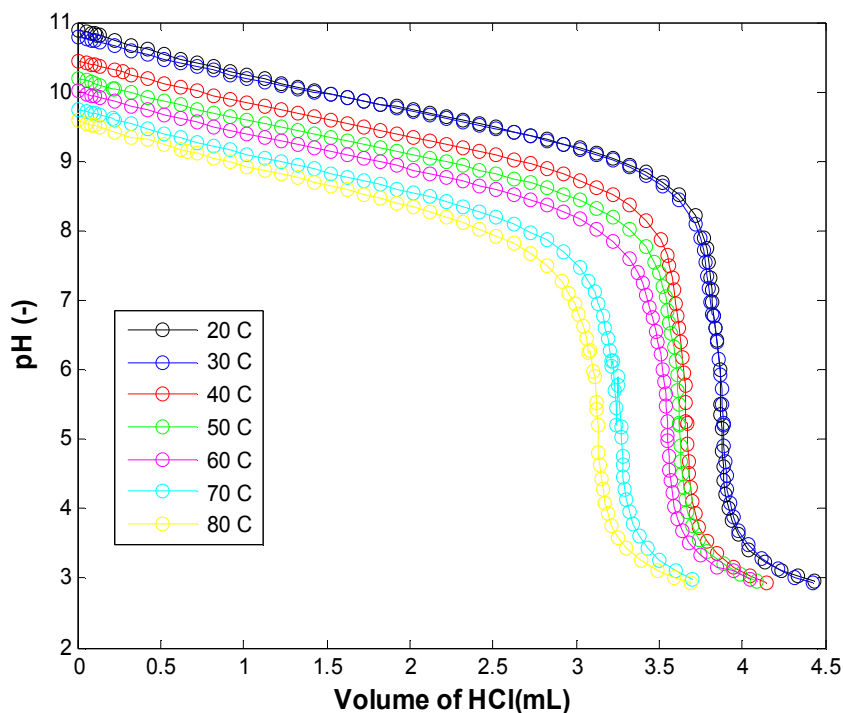


Figure 2.2: pH curves of aqueous solution of 0.01M DEEA at different temperatures.

2.2.2 Atmospheric or low pressure VLE apparatus

The VLE apparatus for atmospheric pressure is designed to operate at temperatures up to 80 °C and consists of four 360-cm³ glass flasks. The apparatus placed in a thermostat box is equipped with heater, fan, water bath, mixing feed controller, IR analyzers, condenser and gas phase pump.

The total pressure in the IR analyzer consist of N₂ and CO₂ during calibration and CO₂, H₂O (small amount) along with amine which is DEEA in this case.

A preloaded DEEA solution of 150 cm³ was fed into flask 2. The same amount was also fed into flask 3 and 4, while flask 1 was used a gas stabilizer. The flasks were heated by water and placed in a thermostated box with temperature measured to within ± 0.1 °C. The gas phase was circulated as the temperature reached the desired level, and equilibrium was obtained when the analyzer showed a constant value for the CO₂ volume percent, but it is preferable to look at the voltmeter reading since it is much more sensitive than the analyzer itself. This took around

~10–20 min in the case of DEEA. A liquid sample to be analyzed for CO₂ and amine concentration was then withdrawn from flask 4 and was properly labeled. Figure 2.3 shows the schematic diagram of the apparatus.

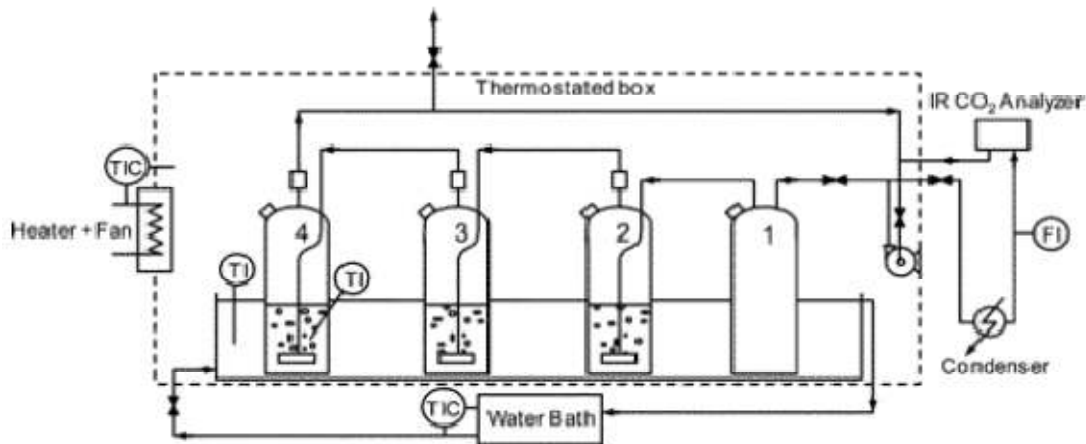


Figure 2.3: Low temperature (atmospheric) equilibrium apparatus (Ma'mun, 2005)

Care was taken during experiment to get minimum amount of condensate especially at higher temperatures.

The IR analyzers used were calibrated each time before using them and there were two analyzers that were used with four channels with each analyzer having two channels of different range as 0-20 %, 0-5 %, 0-1% and 0-2000 ppm(parts per million).

Equilibrium gas phase partial pressures of CO₂ in the system were calculated by the equation

$$P_{CO_2} = y_{CO_2}^{IR} \left[P - (P_{H_2O} - P_{H_2O}^{IR}) - (P_{Am} - P_{Am}^{IR}) \right] \quad (2.1)$$

Where $y_{CO_2}^{IR}$, %CO₂ in the analyzer; atmospheric pressure ; P_{H_2O} and P_{Am} are partial pressures of water and amine at cell 4 temperature while P_{Am}^{IR} and $P_{H_2O}^{IR}$ partial pressure of amine and water at the cooler temperature, Since DEEA is volatile so amine vapour pressure cannot be neglected.

2.2.3 High pressure and high temperature VLE apparatus

Figure 2.4 shows the equilibrium apparatus for DEEA in the rocking equilibrium cell. The apparatus consists of two connected autoclaves (1000 and 200 cm³) which rotate 180° back and forth with 2cm and are designed to operate up to 2MPa and 150 °C. Druck PTX 610 (max 800 kPa) and Schaevitz P 706-0025 (max 2.5 Mpa) pressure transducers, and two k-type thermocouples are used to record pressure and temperature. The apparatus was used for high pressure DEEA test, as at high pressure atmospheric VLE cannot be operated as shown in figure 3.1.

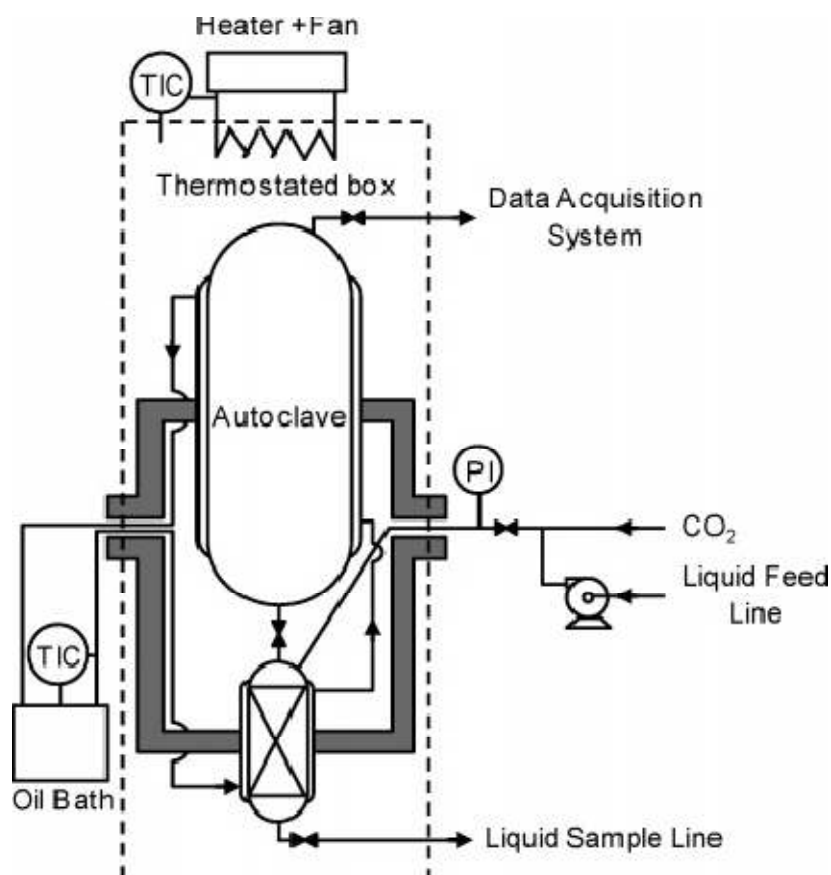


Figure 2.4: High pressure and high temperature VLE apparatus (Ma'mun, 2005)

The autoclave placed in a thermostated box were heated by an oil bath. During heating up the autoclaves were purged with CO₂ several times. The unloaded DEEA (5M or 2M) solution of 200 cm³ was then injected into the smaller autoclave, the amount determined by weight and finally CO₂ was injected to the desired pressure. Equilibrium was obtained when temperature and

pressure was constant to within about ± 0.2 °C and ± 1 kPa. This took approximately 3 to 8 hrs. After equilibrium was obtained, a liquid sample was withdrawn from the smaller autoclave using a 75 cm³ evacuated sampling cylinder where an unloaded DEEA solution of about 50 cm³ was injected into the cylinder before sampling. This was to ensure that all CO₂ in the liquid sample was totally absorbed. The cylinder was then cooled to ambient temperature. The partial pressure of CO₂ was measured by subtracting the partial pressures of water and DEEA from the total pressure. But for the modelling total pressure was used. A comparison between Real vapour pressure and Raoult's law will be presented in results and discussion.

2.2.4 CO₂ analysis and amine analysis of liquid samples

Liquid samples containing CO₂ were analyzed by the precipitation titration method. The liquid sample was added to a 250 cm³ Erlenmeyer flask containing 50 cm³ sodium hydroxide (NaOH, 0.1 N) and 25 cm³ barium chloride (BaCl₂, 0.1 N) solutions. The amount of the liquid sample added dependent on the total CO₂ content in the sample. The Erlenmeyer flask was heated to enhance the barium carbonate (BaCO₃) formation and then cooled to ambient temperature. The mixture was filtered with a 0.45 µm Millipore paper and washed with deionised water. The filter, covered by BaCO₃ was transferred to a 250 cm³ beaker. Deionised water, 100 cm³ was added into the beaker, and enough hydrochloric acid (HCl, 0.1N) was also added to dissolve the BaCO₃ cake. The amount of HCl not used to dissolve BaCO₃ was then titrated with 0.1 N NaOH in an automatic titrator (Metrohm 702 Sm Titrino) with an end point of pH 5.2. Due to possible solvent losses during operation at High temperatures, the DEEA concentrations were determined by titration. A liquid sample of 0.5 cm³ was diluted in 75 cm³ deionised water and titrated with 0.2 N sulphuric acid (H₂SO₄) using the metrohm 702 SM Titrino. The end point was obtained at pH 3 – 4. The DEEA concentrations were found and these concentration were used for getting loading (mol CO₂/ mol amine). Since it is expected to have some amine losses that is why it is necessary to calculate the amine concentration as well.

2.3 Calibration of analyzers

2.3.1 High pressure equipment

For high pressure equipment since the thermocouple and pressure transducer was calibrated once so it's not necessary to be calibrated every time and those calibration data is already fed into computer which was selected before starting the software Labview.

2.3.2 Low pressure equipment

All analyzers were calibrated every time before using such analyzers. The actual concentrations of CO₂ were obtained from the calibration curve drawn for actual CO₂ vol % vs voltage of IR analyzer as shown in figure 2.5.

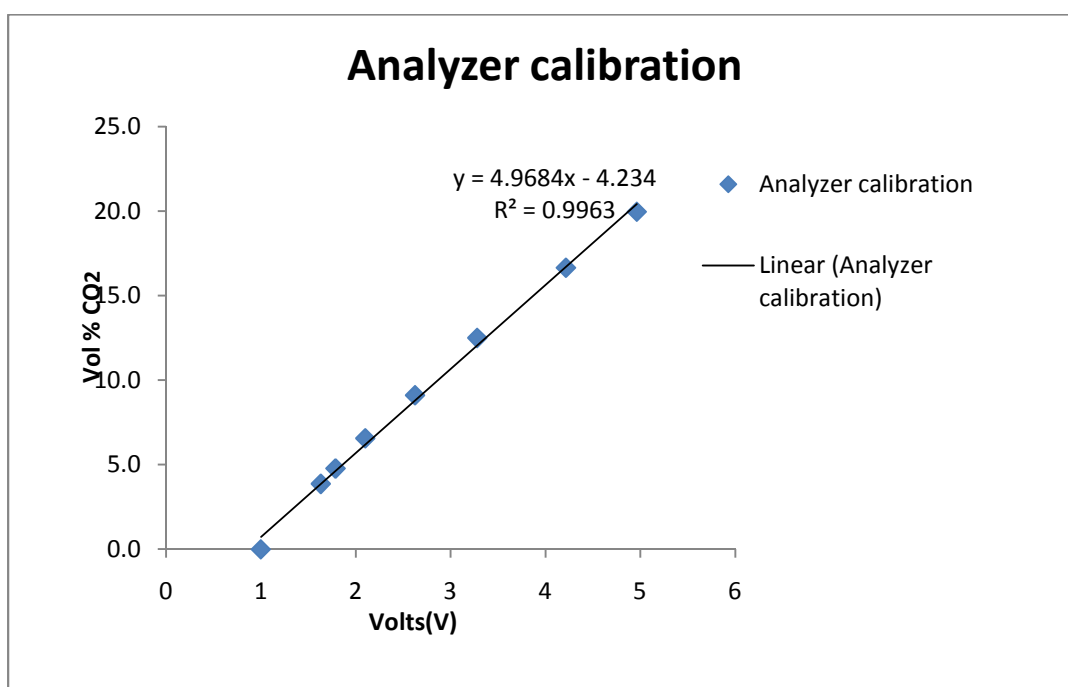


Figure 2.5: Analyzer Calibration

Figure 2.5 shows an example for analyzer calibration and the equation of the line which is basically used to calculate error free Vol% CO₂.

All the observations and CO₂ analyses along with amine analyses were put in an excel sheet to calculate the CO₂ loading as mol of CO₂/mol of amine which will be discussed in results and discussion. The partial pressure of CO₂ was calculated by subtracting partial pressures of water and amine at given temperature from the atmospheric pressure obtained from barometer.

3.0 Experimental results and discussion

Vapor-liquid equilibrium(VLE) experiments were performed for different concentration of DEEA (5M and 2M) in both high pressure VLE and atmospheric VLE at temperatures 40, 60 and 80 °C with atmospheric VLE and 80,100 and 120 °C with high pressure VLE(Vippe).

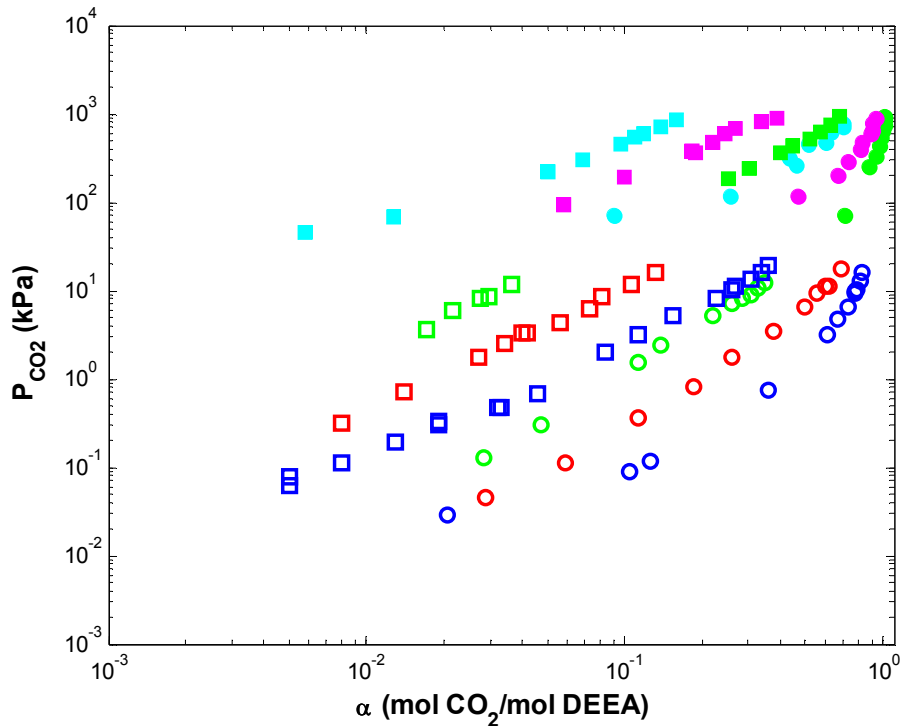


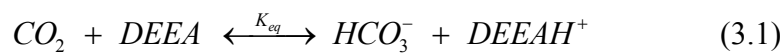
Figure 3.1: DEEA 5M and 2M equilibrium data P_{CO_2} (kPa) as a function of loading. (\square , 40 °C DEEA 5M, \square :60 °C DEEA 5M; \square , 80 °C DEEA 5M ; \blacksquare , 80°C DEEA 5M vippe; \blacksquare , 100°C DEEA 5M vippe; \blacksquare , 120°C DEEA 5M vippe ; \circ , 40°C DEEA 2M; \circ , 60°C DEEA 2M; \circ , 80°C DEEA 2M;; \bullet , 80°C DEEA 2M vippe; \bullet , 100°C DEEA 2M vippe; \bullet , 120°C DEEA 2M vippe).

Data generated with both apparatuses is shown in figure 3.1. Experiments were done with great care and determination. It is evident from the figure 3.1 by looking shows that the data is remarkable both in terms of trend and reproducibility. There is no data available to compare with but still it is possible to tell about the quality of the data. Trends are good and since some of the points were repeated twice which may not be possible to see because they lay one on another and data from both the apparatuses show a trend. Moreover data from atmospheric VLE at 80 °C

agree with data from High pressure VLE (Vippe) at same temperature for both concentration which gives another clue about the quality of data as can be seen in figure 3.1. During experiments some condensate was collected but since amount was fairly less around 0.5 ml which is comparable to the total volume of amine during experiment as approximately 450 ml so it's not possible to calculate CO₂ loading with such a small sample.

It is a good property that DEEA covers a whole range of loading starting with fairly low 0.005 mol CO₂/mol amine to the maximum value of 1 mol CO₂/mol amine as can be seen in figure 3.1. The experiments were not performed to with very low channel analyzers from because as can be seen from figure 3.1 there is not much CO₂ left in the liquid phase specially with 5 molar . Since DEEA is a tertiary amine which makes them capable to absorb more CO₂ per mole amine but on the other hand they react very slowly because they have no carbamate formation like MEA for instance. Having high capacity, low heat of reaction and low heat requirement for regeneration makes it a suitable candidate for CO₂ capture, but using aqueous solution of DEEA without any promoter is a bit difficult as DEEA is slow in reaction if used makes the size or height of absorption tower extremely tall, so in that case tertiary amines like DEEA are generally used with promoters to enhance the reaction rate at certain level in order to have balance between absorption and regeneration. But apart from these benefits it has high vapor pressure having low density and high activity makes it susceptible to solvent loss, which means high load on water wash unit.

According to figure 3.1 it can be seen that the difference between P_{CO₂} is relatively high between



$$P_{CO_2} = \frac{[HCO_3^-][DEEAH^+]}{K_{eq}[DEEA]} \quad (3.2)$$

$$P_{CO_2} = \frac{m \alpha}{K_{eq}(1 - \alpha)} \quad (3.3)$$

5M and 2M based on loading. This can be explained on the basis of equation 3.1, 3.2 and 3.3. For amines without carbamate formation P_{CO₂} is proportional to amine concentration (m), which is

true because by looking at figure 3.1 it is clear that with DEEA 5M partial pressure of CO₂ is much high than DEEA 2M based on amount of CO₂ in liquid phase. It means P_{CO₂} is dependent on amine concentration with no carbamate formation.

Basically it was the idea to calculate and compare vapor pressure from ebulliometer with UNIQUAC and Raoult's law, it is because Raoult's law is for ideal solutions and to use Raoult's law there are some circumstances that must be fulfilled for example enthalpy of mixing is zero or the interaction between the molecules is same regardless of size and shape of molecules in a solution. In terms of activity coefficient.

$$P_{Solution}^{Raoult's\ Law} = x_{DEEA} \cdot P_{DEEA}^{\circ} + x_{H_2O} \cdot P_{H_2O}^{\circ} \quad (3.4)$$

$$P_{Solution}^{UNIQUAC} = \gamma_{DEEA} \cdot x_{DEEA} \cdot P_{DEEA}^{\circ} + \gamma_{H_2O} \cdot x_{H_2O} \cdot P_{H_2O}^{\circ} \quad (3.5)$$

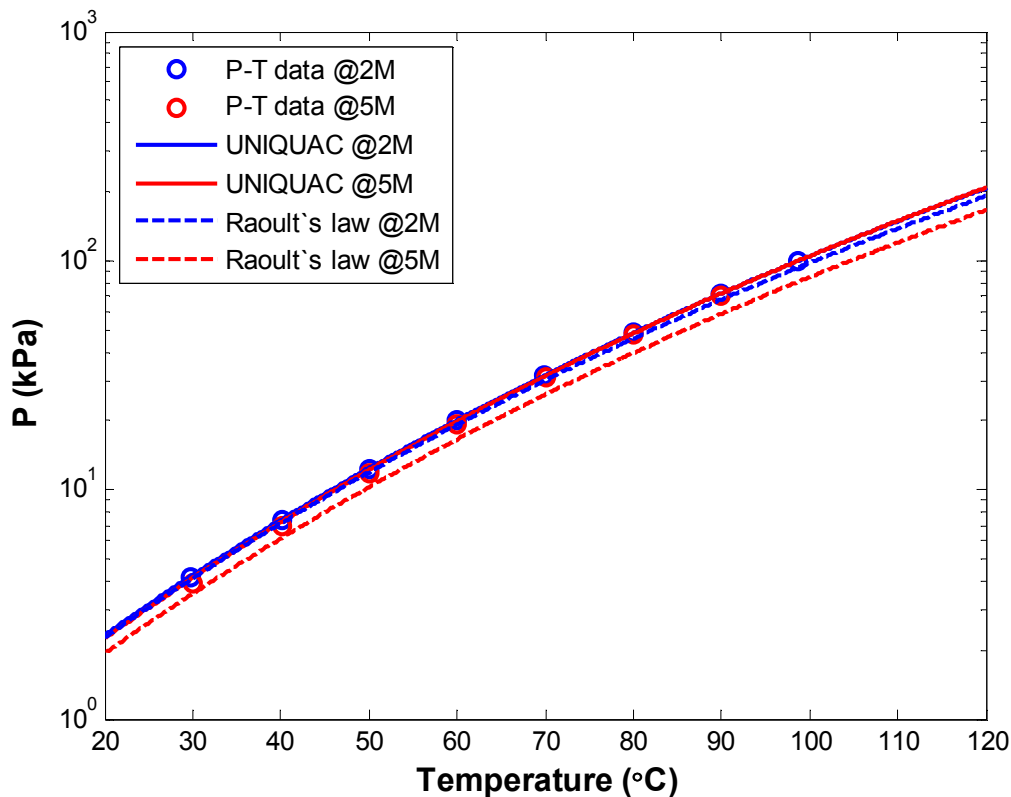


Figure 3.2: DEEA 5M and 2M vapor pressure comparison

It was found that Raoult's law deviates from experimental data as shown in figure 3.2 but on the other hand predictions with UNIQUAC is better because it accounts non-idealities in the form of activity co-efficient.

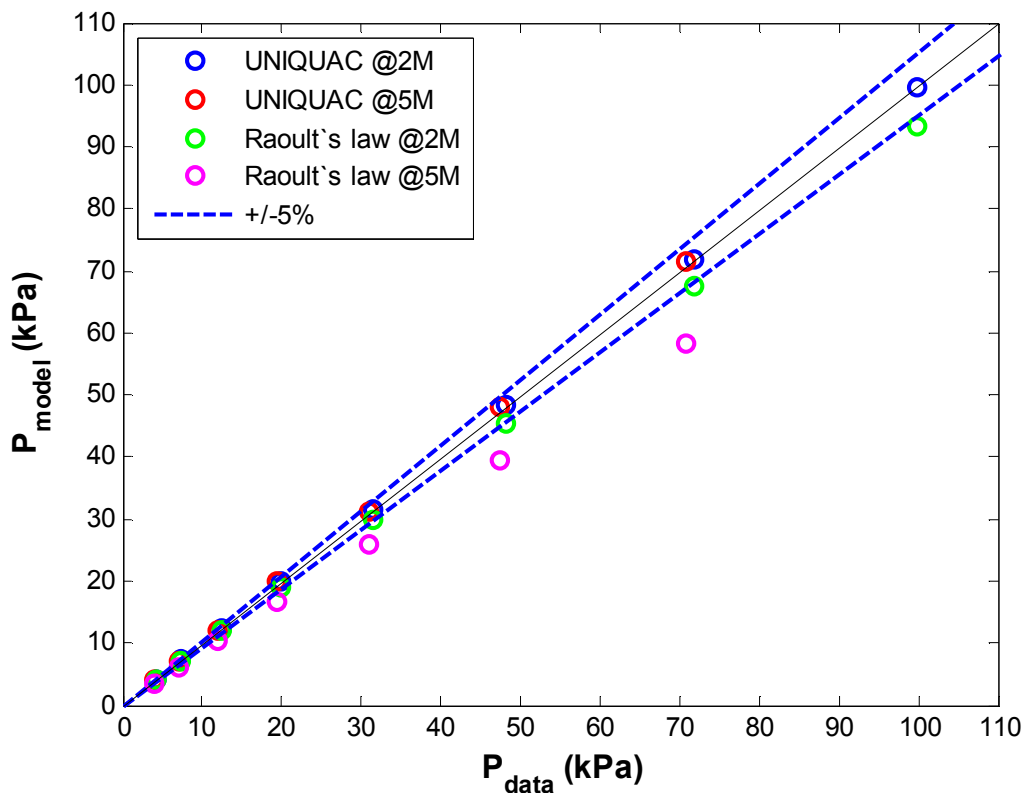


Figure 3.3: Parity plot and deviation

The parity plot in figure 3.3 shows the calculated deviation which increases with increase in temperature. In case of DEEA it showed a deviation of 5 % up till temperature range of experiment around 100 ° C, this could be different for other aqueous solution of amines. The purpose of this discussion is to make people aware that it's always not right to use Raoult's law depending on the type of solvent (physical properties) used and concentration.

3.1 Dissociation constant or pKa results

pKa values obtained from this work were compared with literature data as shown in figure 3.4. As it is evident from the figure that this work is consistent with Hamborg & Versteeg(2009).

The deviation between Little et al (1990) and Hamborg & Versteeg (2009) is 2.06 %.(Hamborg et al, 2011).It shows that the deviation between this work and Hamborg & Versteeg must be less than 2.06 % based on the figure 3.4.

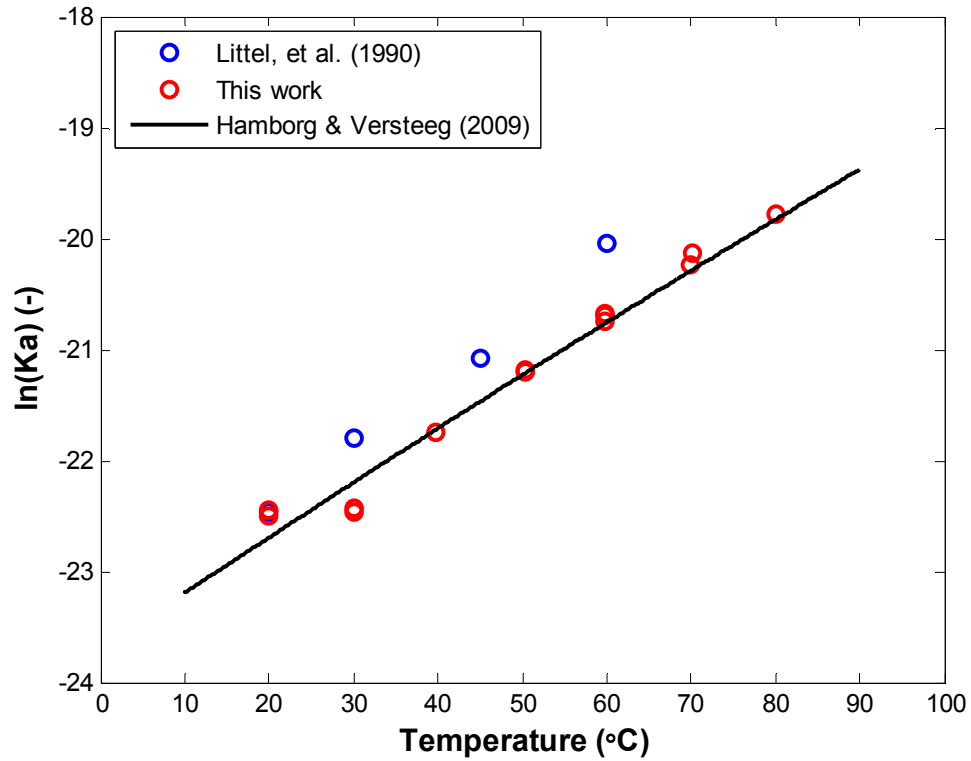


Figure 3.4: K_a values comparison with literature data

4.0 Thermodynamic framework

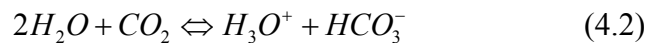
4.1 The equilibria involved

The absorption of CO₂ in aqueous amine solutions involves a quite complex set of equilibrium phase reactions. Below, the reaction scheme for CO₂ and an aqueous alkanolamine solution is given. R₁R₂NH denotes a generic amine, if for example R₁ is –C₂H₄OH and R₂ is H, the amine is monoethanolamine(MEA) which is the most commonly used amine for gas sweetening. The reaction scheme is more or less similar for all types of amines, but there are some differences. For instance for tertiary amines such as DEEA not to form carbamate R₁R₂NCOO[–]. (Hessen E.T, 2010)

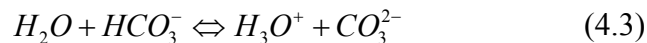
Water ionization:



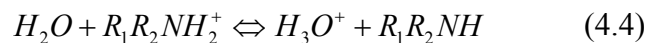
Dissociation of dissolved carbon dioxide:



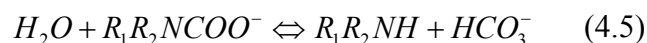
Dissociation of bicarbonate:



Dissociation of protonated amine:



Carbamate to bicarbonate formation only forms in primary amines



From the reaction mechanism it can be seen that the system comprises of both neutral molecules and electrolyte species. The presence of ions makes the modeling non-trivial due to the strong long range interaction between these species. These interactions lead to large non-idealities. Another challenging feature of this ternary system is that it changes character as CO₂

is absorbed into the liquid phase. At low loading the system mainly consists of molecular species and short range forces dominate. As more CO₂ is absorbed; electrolytic compounds are formed and long-range forces will become more prominent. This character change constitutes one of the main challenges for the development of thermodynamic models for the systems in discussion. Also relatively high number of species complicates the modeling. (Hessen E.T, 2010)

Finding the speciation of the system at a given temperature and initial concentration of CO₂ and amine is a chemical equilibrium problem. This problem may be formulated as finding the global minimum Gibbs energy, subject to material balance constraint. (Hessen E.T, 2010)

$$\min_{n \in \Omega} G(n) = \min_{n \in \Omega} (n \mu^T) \quad (4.6)$$

In this equation n is a composition vector and μ is a vector containing the chemical potential of the species. In addition to the chemical equilibria the distribution of species between the vapor and liquid phase must be determined, namely the vapor-liquid equilibria (VLE). The standard VLE problem may be formulated as

$$\mu_i^{vap} = \mu_i^{liq} \quad (4.7)$$

Where μ_i^{vap} and μ_i^{liq} are the chemical potentials of the species i in the vapor phase and liquid phase respectively. Figure 4.1 shows the equilibria involved in the absorption process.

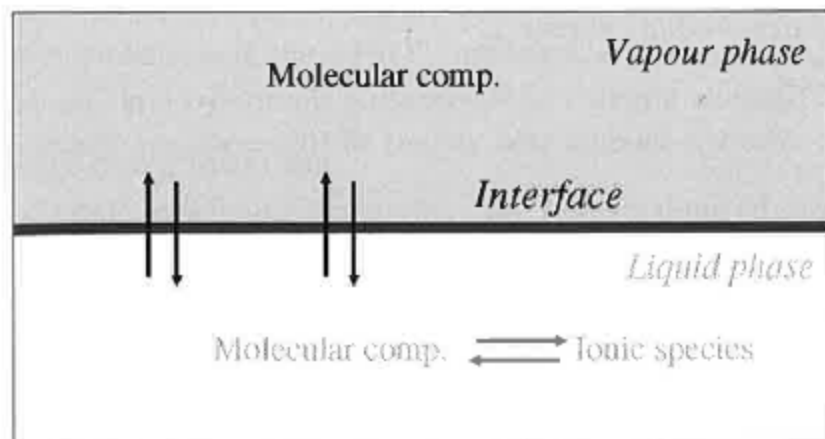


Figure 4.1: Chemical and phase equilibria (Hessen E.T, 2010)

4.2 The extended UNIQUAC model

Sander et al. (1986) presented an extension to the original UNIQUAC model (Abrams and Prausnitz, 1975) by adding an electrostatic term. The model consists of three terms: a combinatorial term, a residual and the electrostatic term of Debye-Hückel type. The model treated here is that of Thomsen et al. (1996), Thomsen (1997) and Thomsen and Rasmussen (1990). **(Hessen E.T, 2010)**

$$g^E = g_c^E + g_r^E + g_{D-H}^E \quad (4.8)$$

The combinatorial term is independent of temperature and is dependent only on the size of the species.

$$\frac{g_c^E}{RT} = \sum_i x_i \ln \left(\frac{\phi_i}{x_i} \right) - \frac{z}{2} \sum_i (q_i x_i) \ln \left(\frac{\phi_i}{\theta_i} \right) \quad (4.9)$$

Where the coordination number is the number of the nearest neighbors around a central solvent molecule, z is the set equal to 10. ϕ_i is the volume fraction, and θ_i is the surface area of the fraction of the component i .

$$\phi_i = \frac{x_i r_i}{\sum_{\forall i} x_i r_i} ; \theta_i = \frac{x_i q_i}{\sum_{\forall i} x_i q_i} \quad (4.10)$$

The model parameters r_i and q_i are the volume and surface parameter for the component i . These parameters may be calculated from non-electrolyte molecules, but the best results are obtained if the parameters are fitted to experimental data (Thomsen, 2006). **(Hessen E.T, 2010)**

The residual term is due to energetic interactions between the molecules and is given by

$$\frac{g_r^E}{RT} = - \sum_i x_i q_i \ln \left(\sum_k \theta_k \psi_{ki} \right) \quad (4.11)$$

The parameter ψ_{kl} is given by

$$\psi_{kl} = \exp\left(\frac{u_{kl} - u_{ll}}{T}\right) \quad (4.12)$$

u_{kl} and u_{ll} are the temperature dependent binary interaction parameters. The activity coefficient expressions of the UNIQUAC model are given by. **(Hessen E.T, 2010)**

$$\ln \gamma_i^c = \ln\left(\frac{\phi_w}{x_i}\right) + 1 - \frac{\phi_i}{x_i} - \frac{z}{2} q_i \left[\ln\left(\frac{\theta_i}{\phi_i}\right) + 1 - \frac{\phi_i}{\theta_i} \right] \quad (4.13)$$

$$\ln \gamma_i^{c,\infty} = \ln\left(\frac{r_i}{r_w}\right) + 1 - \frac{r_i}{r_w} - \frac{z}{2} q_i \left[\ln\left(\frac{r_i q_w}{r_w q_i}\right) + 1 - \frac{r_i q_w}{r_w q_i} \right] \quad (4.14)$$

$$\ln \gamma_i^r = q_i \left[1 - \ln\left(\sum_k \theta_k \psi_{ki}\right) - \sum_k \frac{\theta_k \psi_{ik}}{\sum_l \theta_l \psi_{lk}} \right] \quad (4.15)$$

$$\ln \gamma_i^{r,\infty} = q_i (1 - \ln \psi_{wi} - \psi_{iw}) \quad (4.16)$$

The activity coefficient expressions for the UNIQUAC framework are significantly simpler than the corresponding expressions in the e-NRTL framework. Another positive feature of UNIQUAC based model is the fact that the same activity coefficient expression may be employed for cations, anions and molecular species. The parameter structure of the UNIQUAC model is also simpler than what is the case for the e-NRTL models. These features make UNIQUAC based models far easier to implement than e-NRTL based models. **(Hessen E.T, 2010).**

4.3 Activity coefficient model

The original non-electrolyte equation by Abrams and Prausnitz (1975) was extended for electrolyte systems by addition of an electrostatic term by Sanders et al. (1986) to a modified UNIQUAC equation. The model consists of three terms: a combinatorial, entropic; a residual, enthalpic (short range terms) and the electrostatic (long range) term of Debye-Hückel type. The

model requires volume, r and surface area, q parameters for each species and adjustable binary interaction energy parameters u_{ki} for each pair of species (Aronu et al, 2011). The temperature dependence of interaction energy parameters (ψ_{ki}) of the residual term is given as

$$\psi_{ki} = \exp\left(-\frac{u_{ki} - u_{ii}}{T}\right) \quad (4.17)$$

Where

$$u_{ki} = u_{ki}^0 + u_{ki}^T(T - 298.15) \quad (4.18)$$

4.4 Parameter regression

In DEEA/H₂O/CO₂ system 8 species are involved excluding carbamate. Total number of parameters involved is 88, of which 68 were used from references and 20 were fitted in this work. Table 4.1, 4.2 and 4.4 shows how many parameters were fitted and how many were from literature.

For r and q refer equation 4.10

Species	r	q
H_2O		
DEEA		
CO ₂		
H ₃ O ⁺		
DEEAH ⁺		
OH ⁻		
HCO ₃ ⁻		
CO ₃ ²⁻		

Table 4.1: UNIQUAC volume, r and surface area, q parameters

Grey: Fitted in this work, **Green:** possible parameter obtained from literature

For interaction energy parameters refer equation 4.18.

	H_2O	$DEEA$	CO_2	H_3O^+	$DEEAH^+$	OH^-	HCO_3^-	CO_3^{2-}
H_2O								
$DEEA$								
CO_2								
H_3O^+								
$DEEAH^+$								
OH^-								
HCO_3^-								
CO_3^{2-}								

Table 4.2: UNIQUAC interaction energy parameter for $u_{ij} = u_{ij}^0 + u_{ij}^T(T - 298.15)$; $u_{ij}^0 = u_{ji}^0$

Grey: Fitted in this work, **Green:** possible parameter obtained from literature

	H_2O	$DEEA$	CO_2	H_3O^+	$DEEAH^+$	OH^-	HCO_3^-	CO_3^{2-}
H_2O								
$DEEA$								
CO_2								
H_3O^+								
$DEEAH^+$								
OH^-								
HCO_3^-								
CO_3^{2-}								

Table 5.2: UNIQUAC interaction energy parameter for $u_{ij} = u_{ij}^0 + u_{ij}^T(T - 298.15)$; $u_{ij}^T = u_{ji}^T$

Grey: Fitted in this work, **Green:** possible parameter obtained from literature

4.5 Thermodynamic parameters

Reactions for DEEA can be written as

Water ionization:



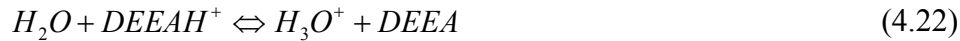
Dissociation of dissolved carbon dioxide:



Dissociation of bicarbonate:



Dissociation of protonated amine:



Thermodynamic parameters needed for each of the models are parameters in the activity coefficient and equilibrium constant. The equilibrium constants are defined in terms of mole fractions, thus they are dimensionless. In this project the equilibrium constant for DEEA was calculated and for other reactions it was used from literature. The temperature dependencies of equilibrium constants are gives as

$$\ln K = C_1 + C_2 / T + C_3 \ln T + C_4 T \quad (4.23)$$

Reaction	Parameter	C_1	C_2	C_3	$10^4 C_4$	$T(^{\circ}C)$	Sources
4.20	K_{H_2O}	132.899	-13445.90	-22.4773	0	0-225	Edwads et al.(1978)
4.21	K_{CO_2}	231.465	-12092.10	-36.7816	0	0-225	Edwads et al.(1978)
4.22	$K_{HCO_3^-}$	216.049	-1231.70	-35.4819	0	0-225	Edwads et al.(1978)
4.23	K_{DEEA}	-165.26	2616.24	23.53	0	0-80	Hamborg & Versteeg, 2009

Table 4.1: Mole fraction based temperature dependent equilibrium constants.

5.0 Modeling results and discussion

5.1 Binary DEEA-H₂O system

For the fitting of ternary data it is mandatory to have binary interaction parameters in order to reduce number of parameter that must be tuned. Binary interaction parameter for DEEA-H₂O system was calculated from Experimental data from ebulliometer. The consistency of binary data is important to be implemented on the ternary system.

Consistency of the binary system can be checked by looking at the trends and comparing with model predicted values. Many parameters are considered which include excess enthalpy (H_E) in kJ/mol, activity coefficient, Pxy and Tx diagrams.

It is necessary to calculate binary interaction parameter, binary parameter will help in reducing number of parameter that must be fitted for ternary system for instance in e-uniquac. The binary parameters which are used later for ternary system are r (DEEA), q (DEEA), u_0 (H₂O-DEEA), u_t (H₂O-DEEA), u_0 (DEEA-DEEA) and u_t (DEEA-DEEA).

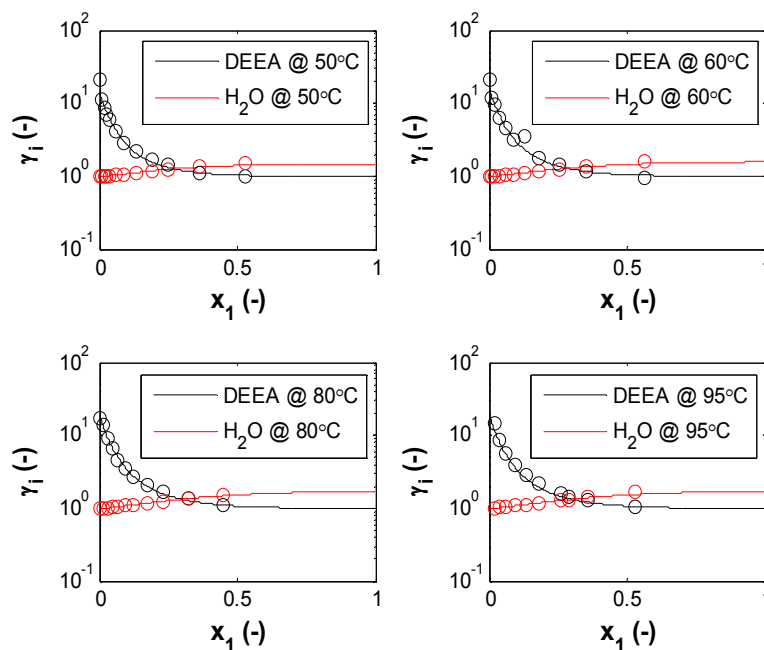


Figure 5.1: H₂O-DEEA activity coefficient, ○ experimental data (red and black), – UNIQUAC (red and black)

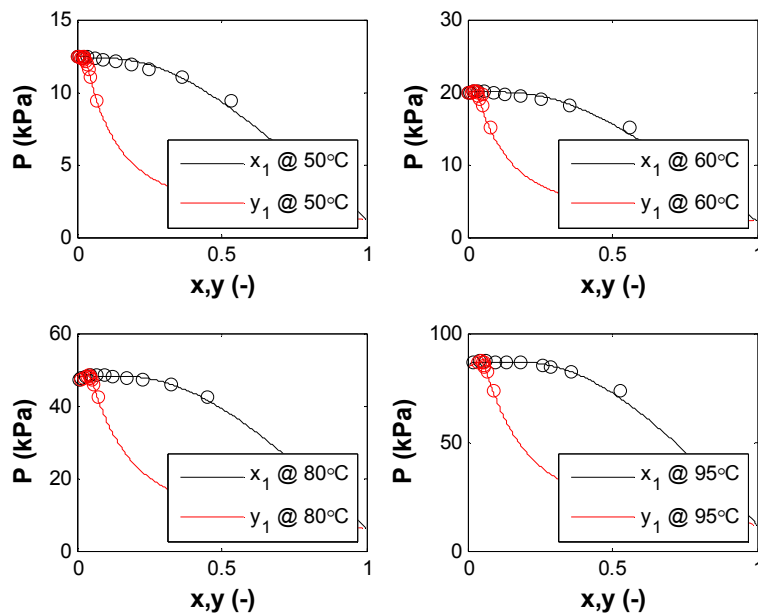


Figure 5.2: Pxy diagram for DEEA at different temperature °C, ○ experimental data (red and black), – UNIQAC (red and black)

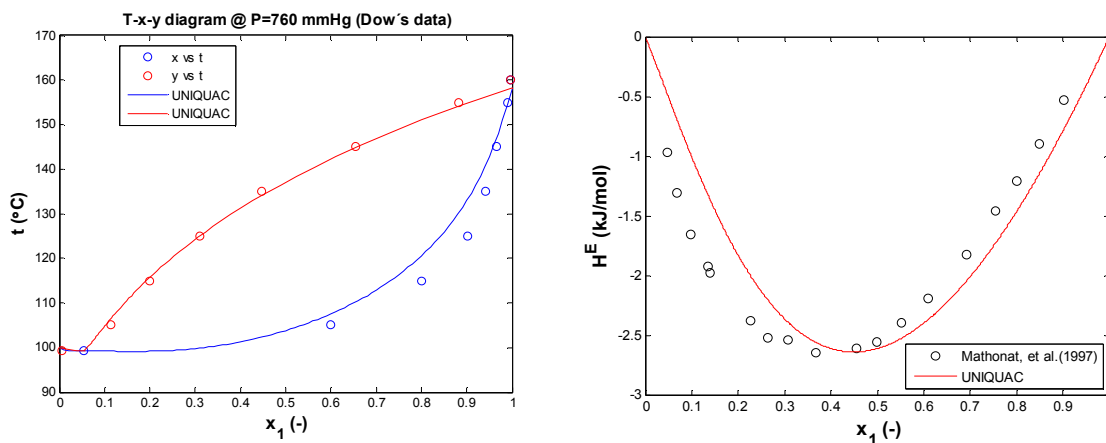


Figure 5.3: Tx diagram for DEEA compared with DOW'S data (left), Excess enthalpy comparison with Mathonat et al, 1997. (Right)

Figures 5.1, 5.2 and 5.3 show the fit between experimental data and the model predicted values. The prediction by the model matches well with experimental data. In figure 5.3 the data from UNIQAC is compared with DOW's data and the results are really good.

Excess enthalpy calculated by UNIQUAC is compared with Mathonat et al (1997), there is still some deviation between the predicted value and the reference value but still the deviation is acceptable.

5.2 Ternary CO₂- DEEA-H₂O system

Experimental data for the 2M and 5M DEEA is later on fitted with e-UNIQUAC at different temperatures 40,60,80,100 and 120°C. Along with that AARD is calculated for the modeled data. The model parameter that need to be evaluated were r , the surface area parameters, q , as well as interaction energy parameters u_{ki}^o and u_{ki}^T . The dataset used for regression of model parameters are; the experimental determined CO₂ partial pressures and total pressure measurement for this work. Regression was difficult with some problems. The first step was to retain as many literature data as possible. During the regression of data the change in behavior of e-UNIQUAC was closely observed with change in parameters and acted accordingly. After checking all the parameters they were grouped together and were applied to be optimized by modfit. The regression analysis was performed through a Levenberg-Marquardt minimization using the MATLAB based parameter estimation tool, Modfit (Hertzberg and Medjell, 1998). The objective function is given as

$$F = \sum_{i=1}^n \left(\frac{P_{CO_2}^{\text{exp}} - P_{CO_2}^{\text{calc}}}{P_{CO_2}^{\text{exp}}} \right)^2 + \sum_{i=1}^n \left(\frac{P_{\text{tot}}^{\text{exp}} - P_{\text{tot}}^{\text{calc}}}{P_{\text{tot}}^{\text{exp}}} \right)^2 \quad (5.1)$$

The deviation of the model results from the experimental data is given as absolute average relative deviation (AARD) as shown below.

$$AARD = 100\% \cdot \frac{1}{n} \sum_n \frac{|P_{\text{model}} - P_{\text{exp}}|}{P_{\text{exp}}} \quad (5.3)$$

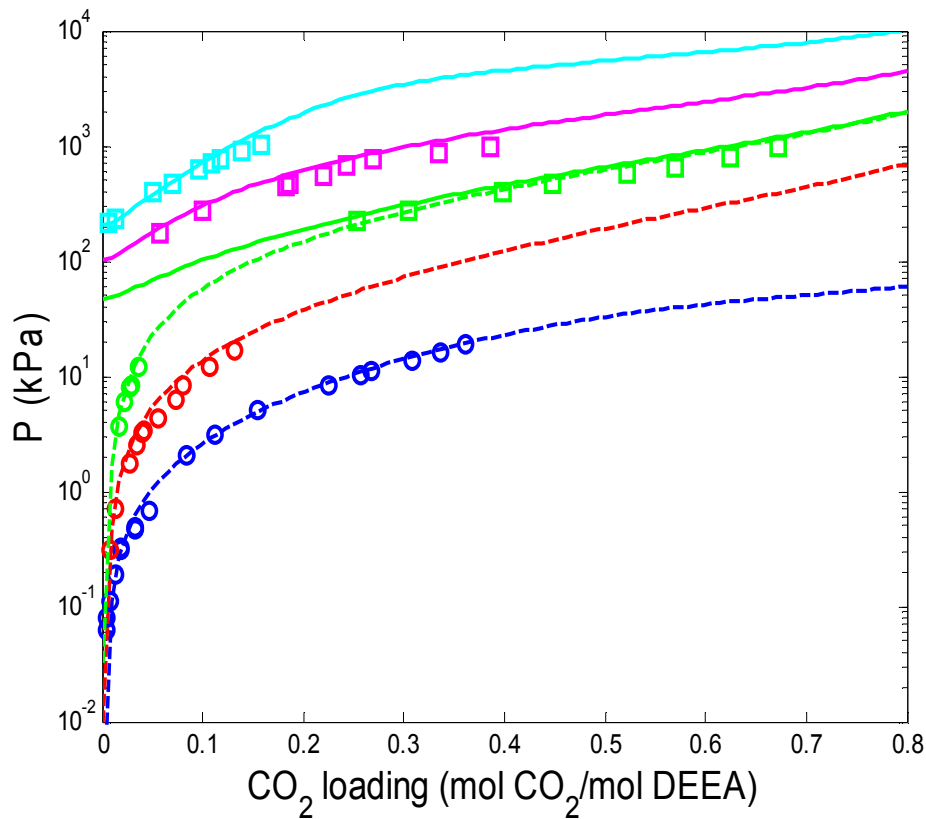


Figure 5.4: DEEA 5M equilibrium data P (kPa) as a function of loading. (\circ , experimental points (P_{CO_2}); \square , experimental points (P_{tot}); Solid lines, e-UNIQUAC(P_{tot}); Dashed lines, e-UNIQUAC(P_{CO_2}); \circ , 40°C; \circ , 60°C; \circ/\square , 80°C; \square , 100°C, \square : 120°C).

Model calculations and experimental CO₂ partial pressures and total pressure from this work as a function of loading and temperature are shown in figure 5.4 and 5.5. It is important to mention here that the data for 80°C in figures 5.4 and 5.5 is basically shown from both low pressure and high pressure with its experimental points and model predictions. In fact the P_{CO_2} is predicted well by the model over DEEA solution of 2M and 5M. There were some problems in regressing the P_{tot} but it still looks good.

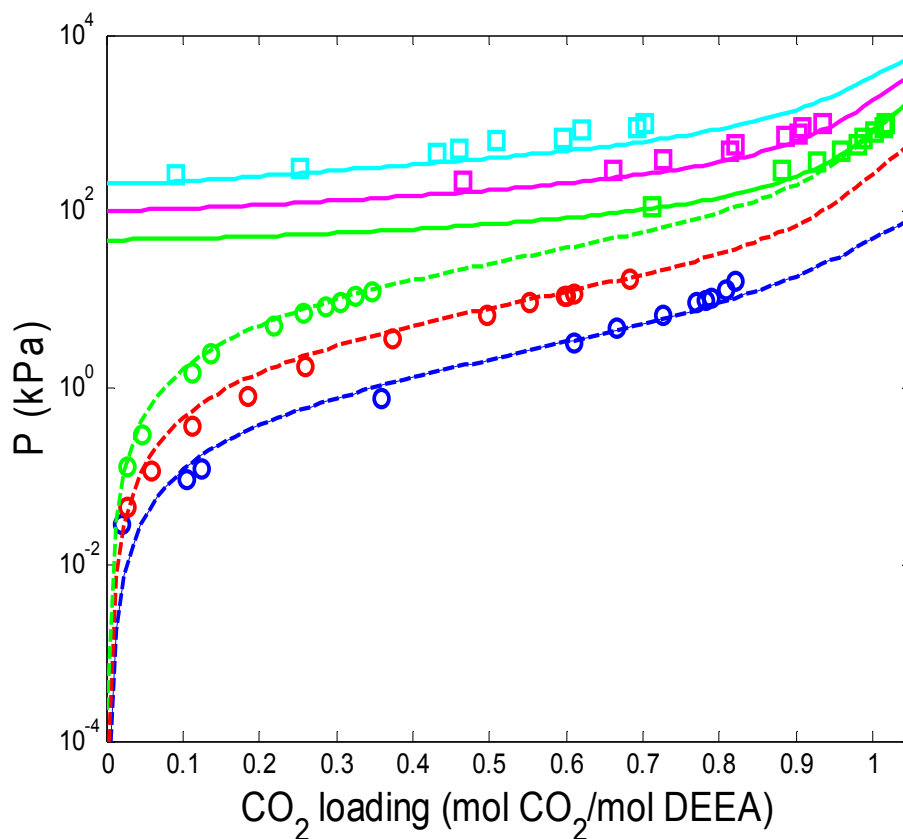


Figure 5.5: DEEA 5M equilibrium data P (kPa) as a function of loading. (\circ , experimental points (P_{CO_2}); \square , experimental points (P_{tot}); Solid lines, e-UNIQUAC(P_{tot}); Dashed lines, e-UNIQUAC(P_{CO_2}); \circ , 40°C; \circ , 60°C; \circ/\square , 80°C; \square , 100°C, \square : 120°C).

The overall absolute average relative deviation (AARD) calculated for this work is 26.5 %.

The parity plots shown in figure 5.6 shows good results especially for P_{CO_2} but for P_{tot} it showed some deviations.

For the modeling of data first it was tuned manually then modfit was applied to make the fit better. There have been some problems like discontinuity in the model from the parameters calculated by modfit, which showed sudden drop of activity coefficient after the discontinuation point which was observed by some other people as well.

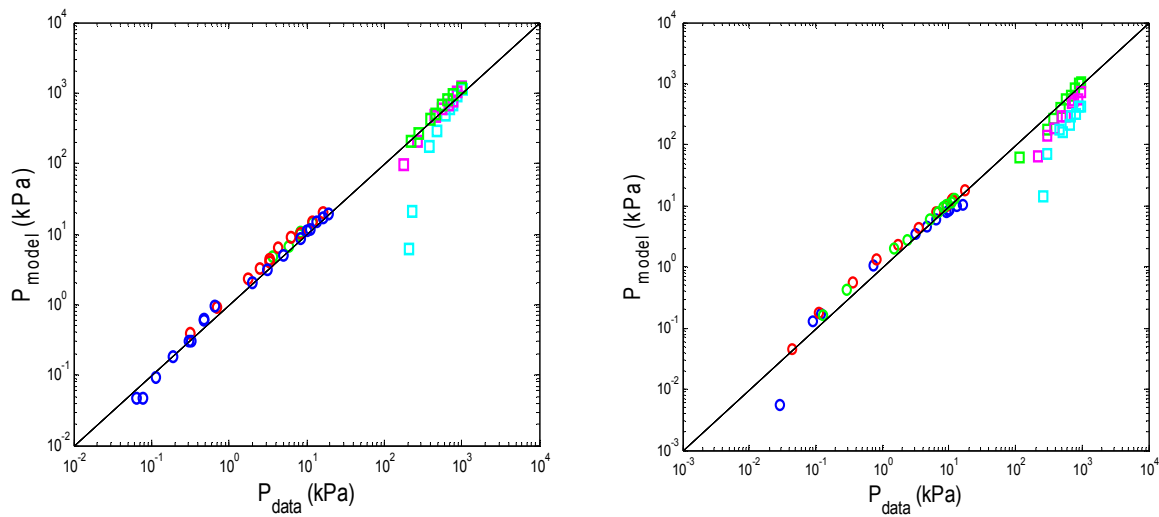


Figure 5.6: DEEA 5M(left) and 2M(right) parity plot between experimental and model predicted pressures (○, 40°C; ○, 60°C; ○/□, 80°C; □, 100°C, □: 120°C).

It would be better to have solubility data for DEEA to help in fitting the data better.

During the calculation it was observed that the pressure contribution from water is much higher than amine especially in DEEA 2M because of large mole fraction of water.

	H_2O	DEEA	CO_2	H_3O^+	DEEAH ⁺	OH ⁻	HCO ₃ ⁻	CO ₃ ²⁻
H_2O	0.0000							
DEEA	-253.79933343	-233.27163666						
CO_2	-137.359	0.0000	40.5176					
H_3O^+	1.0E+04	1.0E+09	1.0E+09	0.0000				
DEEAH ⁺	-417.5551872	3.426629547	-787.8570155	1.0E+09	0.0000			
OH ⁻	600.4952	1.0E+09	2500.0000	1.0E+09	1.0E+09	1562.881 0		
HCO ₃ ⁻	5.17E+02	11942.51274	651.045	1.0E+09	-886.4410536	2500.000 0	2043.432	
CO ₃ ²⁻	361.3877	1.0E+09	2500.000	1.0E+09	1.0E+09	2588.025 0	239.7197	1458.34 40

Table 5.1: UNIQUAC interaction energy parameter for $u_{ij} = u_{ij}^0 + u_{ij}^T (T - 298.15)$; $u_{ij}^0 = u_{ji}^0$

Grey: This work Blue: Aronu et al. (2011b) Green: Thomsen and Rasmussen, 1999;

Brown: Faramarzi et al., 2009.

	H_2O	$DEEA$	CO_2	H_3O^+	$DEEAH^+$	OH^-	HCO_3^-	CO_3^{2-}
H_2O	0.0000							
$DEEA$	-1.53697648	-4.36748945						
CO_2	6.090777	0.0000	13.6290					
H_3O^+	0.0000	0.0000	0.0000	0.0000				
$DEEAH^+$	-0.719030035	-50.23643095	14.70814485	0.0000	0.0000			
OH^-	8.5455	0.0000	0.0000	0.0000	0.0000	5.6169		
HCO_3^-	6.95E+00	-95.2487904	2.773	0.0000	16.50359526	0.0000	17.11482	
CO_3^{2-}	3.3516	0.0000	0.0000	0.0000	0.0000	2.7496	2.611483	-1.3448

Table 5.2: UNIQUAC interaction energy parameter for $u_{ij} = u_{ij}^0 + u_{ij}^T (T - 298.15)$; $u_{ij}^T = u_{ji}^T$

Grey:This work **Blue:**Aronu et al.(2011b) **Green:**Thomsen and Rasmussen,1999;
Brown:Faramarzi et al., 2009.

Species	r	q	Source
H_2O	0.9200	1.4000	Thomsen et al.,1997
$DEEA$	5.13113320	3.03406593	This work
CO_2	5.7410	6.0806	Thomsen and Rasmussen, 1999
H_3O^+	0.13779	1.0E-15	Thomsen et al., 1997
$DEEAH^+$	10.8023836596	6.37474797	This work
OH^-	9.3973	8.8171	Thomsen et al., 1997
HCO_3^-	2.350672	0.749574	Aronu et al.(2011b)
CO_3^{2-}	12.9936	8.6152	Aronu et al.(2011b)

Table 5.3: UNIQUAC volume, r and surface area, q parameters

5.3 Speciation

Speciation data for liquid phase is important in kinetics expressions for mass transfer from gas to liquid phase. Unfortunately in this case there is no NMR (Nuclear Magnetic Resonance) data available for DEEA nor any literature data. NMR data helps in validation of model by comparing model predicted species to that of NMR data at certain loading.

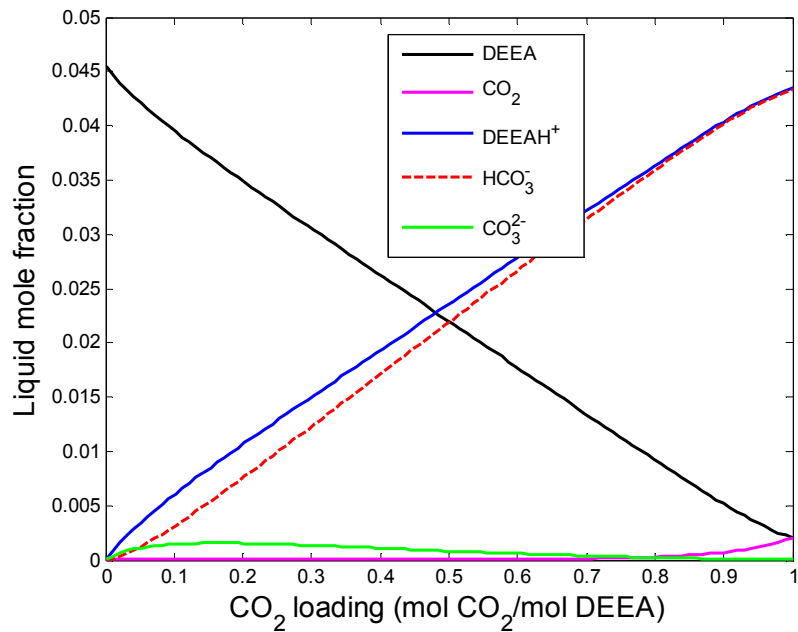


Figure 5.7: DEEA 2M liquid phase speciation at 40°C.

Figure 5.7 and 5.8 shows speciation of 2M and 5M ternary system at 40°C.

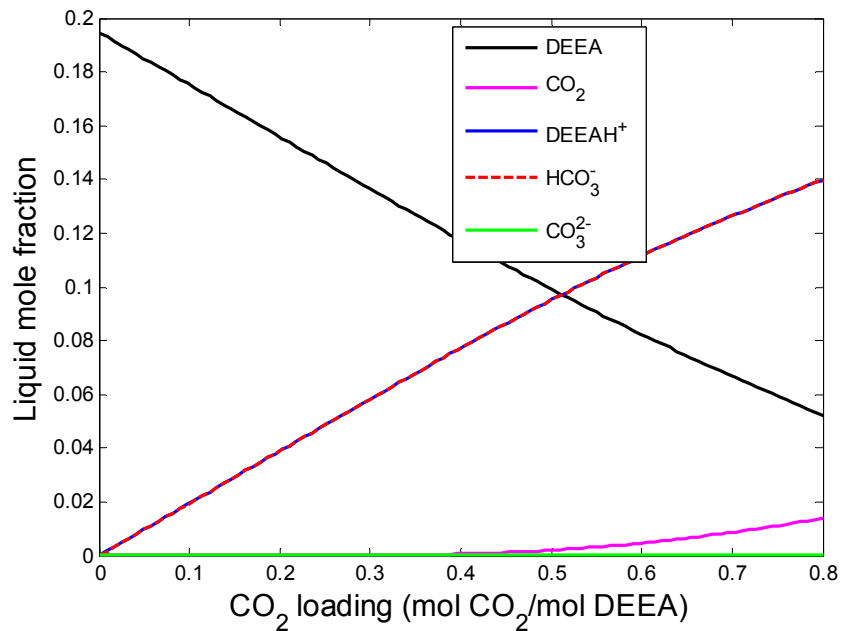


Figure 5.8: DEEA 5M liquid phase speciation at 40°C.

Speciation data based on figure 5.7 and 5.8 seems sensible based on reactions explained in section 4.1. CO₂ is picked by water which is turned into bicarbonate, which means as the loading increases the formation of bicarbonate increases as well in liquid phase. Since the hydronium ion (H₃O⁺) also forms, this H₃O⁺ then reacts with DEEA to form DEEAH⁺, means concentration of DEEAH⁺ also increases with increase in loading. As the solvent saturates the driving force reduces, means liquid phase free CO₂ will increase as shown in figures 5.7 and 5.8. As the loading increases moles of water reduces means carbonate contents reduce as well. Based on figures 5.7 and 5.8 it can be said that flux for 5M has to be less than 2M due to moles of water present or concentration gradient. In case of 5M, protonated DEEA and bi-carbonate goes through same line that is why it's hard to see in figure 5.8.

Conclusions

- Experimental data for vapor-liquid equilibrium of CO₂ in aqueous DEEA solutions are presented for 5M (61.14 wt %) and 2M (23.69 wt %) and from 40 to 120 ° C. CO₂ partial pressures over loaded DEEA solutions were measured using a low temperature equilibrium apparatus while total pressures were measured with high temperature equilibrium apparatus.
- pKa values for DEEA was measured starting with temperature of 20 to 80° C and were with very good agreement with Hamborg and Versteeg(2009) and Little, et al.(1990).
- Ebulliometer data for DEEA 5M and 2M were measured and compared with Raoult's law and UNIQUAC.
- For binary system UNIQUAC is used and e-UNIQUAC for ternary system. In total 20 parameters were fitted in this work.
- Binary interaction parameters were introduced and model predictions were checked with parameters like excess enthalpy, T_x diagram and P_{xy} diagram.
- Data points from atmospheric VLE were regressed as P_{CO₂} whereas for high pressure data points were regressed as P_{tot}.
- Modfit was applied to make the fit better. But sometimes modfit was unable to predict the model after certain loading.
- Average absolute relative deviation (AARD) for the model fit is 26.5 %.
- Parity plots were used to show the deviation between the experimental and model predicted values.

Future recommendations

- It is recommended to have N₂O solubility data for DEEA 2M and 5M, in order to validate the model.
- Availability of NMR data for speciation will help to check the validity of the model predicted values.

References

- Abrams, D.S., Prausnitz, J.M., 1975. Statistical thermodynamics of liquid mixtures. New expression for the excess Gibbs energy of partly or completely miscible systems. *A.I.Ch.E Journal* 21 (1), 116-128.
- Aronu, U.E., Svendsen, H.F., Hoff, K.A., Hessen E.T., Haug-Warberg, T., 2011. Vapor-liquid equilibrium in amino acid salt system: experiments and modeling. *Chemical Engineering science*, 2191-2198.
- Aronu, U.E., Shahla, G., Ardi Hartono., Kristin, G., Lauritsen, Svendsen, H.F., Hoff, K.A., Hessen E.T., Haug-Warberg, T., 2011b. Equilibrium in the H₂O-MEA-CO₂ system: New data and modeling.
- Bolland, O., 2010, Power generation: CO₂ capture and storage (compendium: Process Engineering department: Norwegian University of Science and Technology)
- Dow Chemical (2003), Alkyl Alkanolamines data, Michigan, USA
- Edwards, T.J., Maurer, G., Newman, J., Prausnitz, J.M., 1978. Vapor-liquid equilibria in multi-component aqueous solutions of volatile weak electrolytes. *A.I.Ch.E journal* 24(6), 966-976.
- E. S. Hamborg and G. F. Versteeg. 2009. Dissociation Constants and Thermodynamic Properties of Amines and Alkanolamines from (293 to 353) K. *Journal of Chemical & Engineering data*, 54:1318-1328.
- Faramazi, L., Kontogeorgis, G.M.; Thomsen, K.; Stenby, E.H., 2009. Extended UNIQUAC Model for thermodynamic modeling of CO₂ absorption in aqueous alkanolamine solutions. *Fluid phase equilibria*, 282(2), 121-132.
- Hessen, E. T. 2010; Thermodynamics models for CO₂ absorption. PhD Thesis, Norwegian University of Science and Technology.
- Hertzberg, T., Mejdell, T., 1998. MODFIT for MATLAB parameter estimation in a nonlinear multiresponse model. Norwegian University of science and Technology.
- Kim, I., Andreas, G., Eirik F. da Silva, GHGT 2010, Thermodynamics of Protonation of alkanolamines in aqueous solutions (Poster presentation).

- K. Thomsen. Thermodynamics of electrolyte solutions. Department of Chemical Engineering, DTU, 2006
- Kohl, A.L ; Nielsen, R., 1997. Gas purification; 5th edition.
- Mathonat,C., Majer, V., Mathe, A.E., Grolier J.P.E., (1997). Enthalpies of absorption and solubility of CO₂ in aqueous solutions of methyldiethanolamine.Fluid Phase equil. 140,171-182.
- Ogunlade, D., Heleen de Coninck; Manuela, L., Leo, M., 2005, IPCC Special Report on Carbon Dioxide Capture and Storage. Edited: Bert Metz.
- R.J. Little,M. Bos,and G.J.Knoop.1959:Dissociation constants of some alknolamines at 298,303,318 and 333K.Journal of Chemical & Engineering Data,20:68-82. In German.
- Rackley, S.A., 2010. Carbon Capture and Storage.
- Sander, B., Fredenslund, A., Rasmussen, P., 1986. Calculation of vapor-liquid equilibria in mixed solvent/salt systems using an extended UNIQUAC equation. Chemical engineering science 41(5), 1171-1183.
- Sholeh Ma'mun.2005; selection and characterization of new absorbents for carbon dioxide capture. PhD Thesis, Norwegian University of Science and Technology
- Sartori and Savage. 1983, Sterically hindered amines for CO₂ removal from gases.
- Thomsen, K.1997. Aqueous electrolytes: Model parameter and process simulation. PhD thesis, technical University of Denmark.
- Thomsen, K. Rasmussen, P., 1999. Modeling of vapor-liquid-solid equilibrium in gas aqueous electrolyte systems Chemical Engineering Science, 54(12), 1787-1802.
- Ugochukwu E.Aronu, 2009, Advanced Thermodynamics: With Application to Phase and Reaction Equilibria, KP8108, Project Work.

Acronyms and abbreviations

IPCC	Intergovernmental panel on climate change
DGA	2-(2-aminoethoxy) ethanol
EOR	Enhanced oil recovery
CCS	Carbon Capture and Storage
MEA	Monoethanolamine
DIPA	Di-isopropanolamine
DEA	Di-ethanolamine
TEA	Tri-ethanolamine
MDEA	Methyl di-ethanolamine
AMP	2-amino-2-methyl-1-propanol
PE	2-piperidine ethanol
DEEA	2-(Diethylamino) ethanol
UNIQUAC	UNIversal QUAsiChemical
AARD	Absolute Average Relative Deviation
NMR	Nuclear Magnetic Resonance

List of symbol and units

kPa	Kilo Pascal
MPa	Mega Pascal
R ₁ R ₂ -	Alkyl radical
K_{eq}	Equilibrium constant
x	Mol fraction of liquid phase
y	Mol fraction of gas phase in liquid form
Ω	Material balance constraint
n	Composition vector
μ_i^{vap}, μ_i^{liq}	Chemical potential of species i in the vapor and liquid phase
g^E	Excess Gibbs energy
ψ_{ki}	Temperature dependent interaction energy parameter
γ	Activity coefficient
P_{model}	Model pressure
P_{exp}	Experimental pressure
$P_{CO_2}^{calc}$	Model predicted partial pressure of CO ₂
$P_{CO_2}^{exp}$	Experimental partial pressure of CO ₂
P_{tot}^{exp}	Experimental total pressure

P_{tot}^{calc}

Model predicted total pressure

Appendices

Appendix A1:- P_{CO₂} and P_{tot} data as a function of loading (mol/mol).

DEEA 2M (23.69 wt %)						
40 ° C		60 ° C		80 ° C		
P _{CO₂} (kPa)	α (mol/mol)	P _{CO₂} (kPa)	α (mol/mol)	P _{CO₂} (kPa)	P _{tot} (kPa)	α (mol/mol)
9.2459	0.7716	17.3420	0.684244	12.1118		0.346425
9.8596	0.7821	11.1619	0.599064	10.8077		0.325565
16.0915	0.8215	11.1667	0.600052	9.0419		0.306743
12.9008	0.8105	11.4225	0.611996	8.1541		0.286443
10.3528	0.7905	9.1672	0.552499	7.0192		0.258532
6.5304	0.7268	6.5327	0.497397	5.1604		0.219109
4.7206	0.665	3.5056	0.373231	2.4091		0.137697
3.1936	0.610	1.7360	0.260147	1.5087		0.113054
0.7433	0.36039	0.8166	0.185494	0.2967		0.047122
0.1194	0.12523	0.3645	0.11283	0.1303		0.028265
0.0907	0.104752	0.1121	0.059135	254.2291	299.7	0.882733
0.0288	0.020382	0.0448	0.029015	327.4797	373.1	0.928373
				433.9945	479.6	0.959232
				532.9742	578.6	0.980625
				636.6686	682.3	0.987417
				736.148	781.7	1.003281
				859.4557	905.1	1.015916
				922.4572	968	1.017411
				70.1867	115.7	0.711555
100 ° C			120 ° C			
P _{CO₂} (kPa)	P _{tot} (kPa)	α (mol/mol)	P _{CO₂} (kPa)	P _{tot} (kPa)	α (mol/mol)	
201.8088	299.9	0.662161	114.6947	305.7	0.253878	
293.4663	390.6	0.726559	263.4855	454.4	0.460067	
395.4042	493	0.814303	312.5403	503.6	0.43301	
477.1511	574.5	0.820548	462.6737	653.8	0.508146	
605.3171	702.6	0.887468	484.6118	675.2	0.596392	
653.1955	750.6	0.903138	631.3359	821.9	0.621736	
782.4379	879.7	0.907717	700.1979	891.3	0.701688	
879.7615	977.1	0.935747	775.7734	966.7	0.693006	
118.6146	216.2	0.465791	71.90638	262.7	0.091161	

DEEA 5M (61.14 wt %)						
40 ° C		60 ° C		80 ° C		
P _{co2} (kPa)	α (mol/mol)	P _{co2} (kPa)	α (mol/mol)	P _{co2} (kPa)	P _{tot} (kPa)	α (mol/mol)
19.2247	0.3603	16.4195	0.131	8.3621		0.030
16.1242	0.3359	11.9620	0.106	11.8754		0.036
13.4297	0.3086	8.4398	0.081	8.1390		0.028
11.1739	0.2670	6.2655	0.073	5.8634		0.021
10.2949	0.2573	4.3307	0.056	3.6517		0.017
8.3033	0.2253	3.3247	0.042	357.7141	397	0.398341
5.1141	0.154	3.2840	0.040	426.2157	465.5	0.447366
3.1326	0.112	2.5008	0.034	525.638	564.9	0.522111
2.0242	0.084	1.7490	0.027	623.1317	662.4	0.569398
0.6679	0.046	0.6970	0.014	743.6492	782.9	0.624297
0.4711	0.033	0.3152	0.008	955.8125	995.1	0.672557
0.4827	0.032			238.6145	277.8	0.304095
0.3273	0.019			184.3097	223.5	0.253092
0.3067	0.019					
0.1919	0.013					
0.1125	0.008					
0.0783	0.005					
0.0634	0.005					
100 ° C			120 ° C			
P _{co2} (kPa)	P _{tot} (kPa)	α (mol/mol)	P _{co2} (kPa)	P _{tot} (kPa)	α (mol/mol)	
367.8057	452	0.187029	223.6736	388.6	0.050322	
377.3936	461.6	0.181858	307.1114	472.3	0.069118	
472.3524	556.3	0.219457	454.5271	619.7	0.096043	
587.5966	671.8	0.243243	539.2323	704.4	0.108626	
676.4833	760.5	0.269422	596.7848	761.9	0.117711	
798.3749	882.5	0.335511	721.6271	886.8	0.138401	
908.0141	992.1	0.38616	870.1796	1035.3	0.157802	
189.2742	273.3	0.099843	67.96875	233	0.012662	
92.52309	176.6	0.057679	47.07924	212.1	0.005766	

Appendix A2:-pKa values with different temperatures

Temperature ° C	pKa
20-A	9.747
20-B	9.772
30-A	9.756
30-B	9.741
40-A	9.445
40-B	9.447
50_A	9.201
50_B	9.205
60-A	9.009
60-B	8.991
60-C	8.978
70-A	8.785
70-B	8.746
80-A	8.59
80-B	8.59

Appendix A3:-Activity coefficient model of UNIQUAC used in MATLAB (Ugochukwu E.Aronu, 2009).

$$\ln \gamma_k = \ln \frac{\phi_k}{x_k} + 1 - \frac{\phi_k}{x_k} + \frac{z}{2} q_k \left(\ln \frac{\theta_k}{\phi_k} + \frac{\phi_k}{\theta_k} - 1 \right) + q_k \left[1 - \ln \left(\sum_j \theta_j \tau_{jk} \right) - \sum_i \frac{\theta_i \tau_{ki}}{\sum_j \theta_j \tau_{ji}} \right]$$